

PREDICTING THE PERFORMANCE OF STRUCTURES
IN REGIONS OF HIGH SEISMICITY

by

Joseph Penzien
Professor of Structural Engineering
University of California, Berkeley

SUMMARY

The complete seismic design process of certain important structures based on time-history dynamic analyses is traced from the initial preliminary design stage through the final stage of predicting lifetime performance to strong motion earthquakes. Emphasis is placed upon (1) selection of sound design procedures, (2) consideration of field and laboratory evidence, (3) application of present day knowledge, and (4) recognition of uncertainties involved in the complete process. It is concluded that meaningful predictions of performance can be made only when formulated in a probabilistic sense.

INTRODUCTION

In recent years, the availability of high speed digital computers has dramatically changed methods and procedures used by practicing engineers in designing certain important structures such as nuclear power plants and high rise buildings. Basic knowledge gained from analytical and experimental research and from field investigations can now be applied effectively in developing new and improved seismic resistant designs.

While this change has obviously been beneficial to all concerned, it has raised many questions causing confusion in both the research community and the practicing profession. The author of this paper is of the opinion that many of the problems involved can be brought into much better focus if nondeterministic concepts are used in interpreting research results and in carrying out the design process. At least much of the confusion can be diminished by formally introducing concepts of probability.

It is therefore the main purpose of this paper to trace through the design process of certain important structures based on three-dimensional time-history dynamic analyses where uncertainties are introduced and to point out how they influence predictions of lifetime performance. This process, as shown in Fig. 1, consists of eight stages (1) preliminary design, (2) three-dimensional ground motion definition, (3) mathematical modelling of foundation-structure system, (4) three-dimensional dynamic time-history analysis, (5) interpretation of the results of dynamic analysis in terms of prototype behavior, (6) redesign of structure as needed, (7) assessment of structural safety as designed, and (8) assessment of structural safety as built. The order of these stages has been selected for systematic discussion but they should not be considered independently of each other. The feedback loop from stage No. 6 to stage

No. 3 of the design process is needed only when the design changes in stage No. 6 are significant.

Obviously, this design process is much too complex to be applied to most structures where it is sufficient to use standard code design procedures (stage No. 1, Fig. 1). It should be recognized however that even for these cases, the methodology and concepts presented are helpful to the decision making process leading to good seismic resistant designs and to the assessment of safety against damage or possible collapse.

PRELIMINARY DESIGN

Preliminary design is one of the most important stages during the entire design process as decisions made regarding choice of materials and architectural layout often are major factors affecting the safety and lifetime performance of a structure under seismic conditions. To illustrate this point, several examples will now be considered.

First, let us examine undesirable effects which can result from an irregular layout of a building. Figure 2 shows two modern bank buildings located in Managua, Nicaragua, which experienced the 1972 earthquake⁽¹⁾. On the right side, one can observe the 18-story reinforced concrete Banco de America building which is very regular in geometric form. This desirable shape can be seen in the vertical section and typical floor plan of Figs. 3 and 4, respectively. Although this building suffered some structural and nonstructural damage, its large symmetrically-located, coupled shear walls limited this damage to levels significantly below those observed in more flexible structures. The reinforced concrete Banco Central building on the other hand, shown to the left in Fig. 1, suffered heavy damage. This building had windows on three sides with the fourth side closed by masonry infill walls as shown to the right in Fig. 5. These infill walls combined with the reinforced concrete shear walls around the elevator shafts and stairwells as seen in Fig. 6 introduced an extremely large eccentricity into the building which for transverse excitation will cause large torsional response to develop. Obviously, irregular forms of this type should be avoided whenever possible.

Another example of an irregular building which suffered heavy damage during an earthquake is the Olive View Hospital building shown schematically in an elevation view in Figs. 7 and 8⁽²⁾. During the 1971 San Fernando, California, earthquake, part of the first floor extending outward from the main building collapsed and the first and second stories suffered very large drift deformations (up to 30"). Both of these stories were of the "soft story" design since the shear walls in the upper stories terminated at the second floor level. The upper stories above the second floor level suffered only minor damage during the earthquake.

An examination of the structural design of the Olive View Hospital building reveals large discontinuities in strength, stiffness, and ductility of the columns and girders as shown in Fig. 7. These discontinuities combined with similar discontinuities produced by termination of the upper story shear walls at the second floor were influencing

factors affecting the observed performance of the overall structure. Another significant factor influencing performance was the introduction of a large mass into the system through the placement of a large volume of soil on the first floor at garden level, Fig. 8. Clearly, unnecessary masses and discontinuities of the type mentioned here should be avoided in the preliminary design whenever possible.

A second type of architectural layout which can easily result in poor seismic performance unless special precautions are taken is that type employing deep spandrel beams and short columns as illustrated in Figs. 9 and 10. Failures in this type of structure normally occur in the columns where high shear forces develop as a result of having short column lengths. Since failures of this type are very brittle in nature, high strength must be provided in the structure to insure proper safety against heavy damage or collapse. When selecting this type of structural form, it is well to recall the heavy damage suffered by school buildings of this type during the 1968 Tokachi-Oki earthquake in Japan⁽³⁾. One of these school buildings was reviewed and found to satisfy the earthquake requirements existing at that time for California schools.

Hopefully, these examples are sufficient to stress the importance of considering seismic performance even in the early preliminary design phase when selecting the architectural layout. Obviously, it is desirable for the structural engineer to work closely with the architect during this phase of the overall design process. Once decisions on architectural layout have been completed, the structural engineer will complete the preliminary design phase by sizing and detailing all structural components using equivalent static seismic loads and the elastic design philosophy in compliance with building code provision. In carrying out this phase, the designer should detail the structure for good post-yield performance.

THREE-DIMENSIONAL GROUND MOTION EXCITATION

To carry out three-dimensional time-history dynamic analyses during the design of an important structure, free surface ground motions must be defined for the site. While ground motion at a point actually has six components⁽⁴⁾, 3 translational and 3 rotational, it is usually sufficient to consider only the three translational components.

A very simple approach to defining these three components would be to assume that certain recorded ground motions of a past earthquake are representative of the future site ground motions to be defined. The three accelerograms recorded during the Taft, California, earthquake of 1952 as shown in Fig. 11 are often normalized to the desired intensity level and used for this purpose. One can, of course, question this simple approach as two recorded accelerograms, even for the same site location, often have quite dissimilar characteristics.

Another approach to defining the three translational components of motion is to generate synthetic accelerograms which are derived from a set of prescribed response spectrum curves^(5,6). Two sets of

smooth response spectrum curves (normalized to 1g peak acceleration) now commonly used for this purpose are shown in Fig. 12⁽⁷⁾. These smooth curves which were obtained by a statistical analysis of actual response spectrum curves for many past recorded accelerograms represent mean-plus-one standard deviation levels. Two synthetic accelerograms derived from the smooth design response spectrum curves of Fig. 12 are shown in Fig. 13. The actual response spectrum curves for the synthetic accelerogram of Fig. 13 representing horizontal motion is shown by the solid curves in Fig. 14 where they can be compared with the prescribed design spectra. The differences between these two spectra represent numerical inaccuracies introduced when generating the synthetic accelerogram.

A third approach to defining the three translational components of motion is to use the stochastic model⁽⁸⁾

$$\begin{aligned} a_x(t) &= \zeta(t) b_x(t) \\ a_y(t) &= \zeta(t) b_y(t) \\ a_z(t) &= \zeta(t) b_z(t) \end{aligned} \quad (1)$$

where $\zeta(t)$ is a prescribed deterministic intensity function which converts stationary random processes $b_x(t)$, $b_y(t)$, and $b_z(t)$ to nonstationary processes $a_x(t)$, $a_y(t)$, and $a_z(t)$, respectively. This approach has the distinct advantage that a complete ensemble (or family) of possible accelerograms can be generated for each component of motion.

When generating accelerograms, one is immediately faced with the question of whether or not the separate components should be correlated with each other statistically and, if so, to what degree should they be correlated. In a recent paper, the author discusses this question and shows that statistically correlated ground motions defined by Eqs. (1) can be transformed from the x, y, z orthogonal coordinate system to an x', y', z' orthogonal coordinate system in which the components $a_{x'}(t)$, $a_{y'}(t)$, and $a_{z'}(t)$ are statistically uncorrelated. This transformed system defines a set of principal axes with the mean square intensities of ground motions having maximum, minimum and intermediate values along the major, minor and intermediate axes, respectively. In mathematical terms, the transformed components of motion are related to the original components through the relation

$$\begin{pmatrix} a_{x'}(t) \\ a_{y'}(t) \\ a_{z'}(t) \end{pmatrix} = \begin{bmatrix} \underline{a} \end{bmatrix} \begin{pmatrix} a_x(t) \\ a_y(t) \\ a_z(t) \end{pmatrix} \quad (2)$$

where \underline{a} is the orthogonal transformation matrix. Defining covariance terms

$$\begin{aligned}\mu_{ij} &= \langle a_i(t) a_j(t) \rangle \quad i, j = x, y, z \\ \mu'_{ij} &= \langle a'_i(t) a'_j(t) \rangle \quad i, j = x', y', z'\end{aligned}\quad (3)$$

, where the triangular brackets denote time average, one can establish the corresponding covariance matrices

$$\underline{\mu} = \begin{bmatrix} \mu_{xx} & \mu_{xy} & \mu_{xz} \\ \mu_{yx} & \mu_{yy} & \mu_{yz} \\ \mu_{zx} & \mu_{zy} & \mu_{zz} \end{bmatrix} \quad ; \quad \underline{\mu}' = \begin{bmatrix} \mu'_{xx} & 0 & 0 \\ 0 & \mu'_{yy} & 0 \\ 0 & 0 & \mu'_{zz} \end{bmatrix}\quad (4)$$

It is easily shown that these two covariance matrices are related through the orthogonal transformation matrix equation

$$\underline{\mu}' = \underline{a}^T \underline{\mu} \underline{a} \quad (5)$$

In other words, the covariance matrix transforms exactly like the three-dimensional stress matrix; thus, demonstrating the existence of principal axes. It has been found that the directions of the major and minor principal axes often correlate strongly with direction to the reported epicenter and the vertical direction, respectively. Figure 15 shows directions of the major principal axis for different time intervals t_1 to t_2 during the May 16, 1968 Tokachi-Oki, Japan, earthquake. The lengths of the solid arrows in this figure represent mean square intensities of the major principal motion over the corresponding time intervals. Clearly, the correlation of major principal direction with epicenter direction, as shown by the dashed arrow, is good in this case.

The above transformation and resulting correlation suggest that components of ground motion, as generated, be statistically independent and that the major axis of motion be directed towards the expected epicenter and the minor axis be directed vertically. One may, of course, wish to consider a variety of directions for the prescribed motions corresponding to critical axes of the structural system under consideration, in which case the principal uncorrelated ground motions should be transformed to the desired set of axes by the corresponding orthogonal coordinate transformation. The new set of motions will then be cross correlated properly.

In the above discussion, no mention was made of the influence of local soil conditions on the characteristics of free field surface ground motions. This influence can, of course, be introduced into the above procedures for generating three-dimensional components of ground motion provided it can be quantified in a realistic way. If there is sufficient statistical evidence to warrant it, one can define different smooth design response spectrum curves for different soil conditions; thus reflecting this influence on the generated synthetic accelerograms. Likewise, one can use different filter parameters in the stochastic model, to reflect this same influence on the ensemble of accelerograms obtained.

Deterministic analyses have also been made to attempt to quantify the influence of soil conditions on the free surface ground motions. Most of these studies have used the one-dimensional shear beam model shown in Fig. 16⁽⁹⁾. This shear beam is usually modelled linearly but with the elastic and viscous damping properties adjusted to reflect mean stiffnesses and total energy absorption (hysteretic + viscous), respectively, consistent with the shear strain levels developed. The horizontal acceleration $a_b(t)$ representing bedrock motion is applied at the base of the shear beam and the resulting horizontal surface acceleration $a_d(t)$ is determined from a time-history dynamic analysis. If the soil extends uniformly over a large horizontal distance and if the bedrock is indeed moving in one horizontal direction as a rigid body, one can expect reasonable results from such a model. However, significant departures from these ideal conditions are often present; therefore, the model can be seriously questioned. For example, out-of-phase components of horizontal and vertical motions at point c over those present at point b have an influence on the horizontal surface motions at d . If these out-of-phase components are significant in a distance bc of the same order of magnitude or less than the depth of the soil layer, then the rigid horizontal bedrock motion assumption is no longer valid. It would be most helpful in studying this problem if cross correlations of the components of motions at points b and c were known as a function of the distance bc separating them.

It should be recognized that considerable differences in points of view exist among those who attempt to quantify the influence of local soil conditions on the characteristics of free surface ground motions. Even those adopting similar analytical procedures obtain a wide range of predicted response spectral values for similar site conditions and seismic intensity. Figure 17 is intended to depict this range of values in a qualitative sense only.

From a deterministic point of view, a wide range of predicted spectral values for surface motions under similar conditions may be disturbing. However, in view of the fact that large variations in the response of nonlinear systems can occur with small changes in model parameters or in excitation characteristics, this wide range is acceptable from a nondeterministic point of view. The difference being that now a certain probability of occurrence must be assigned to a given spectral value. Stochastic modelling is therefore attractive from this point of view as the variations are formally recognized in a probabilistic sense.

MATHEMATICAL MODELLING OF FOUNDATION - STRUCTURAL SYSTEM

To carry out a three-dimensional dynamic analysis, an appropriate mathematical model must be established for the complete foundation-structural system. This model should realistically characterize the mass distributions, force-deformation relations, and energy absorption characteristics of the individual elements making up the total system.

Modelling of mass distributions is easily accomplished using the lumped mass procedure indicated by the building model shown in Fig. 18.

Approximating distributed masses in this manner causes no difficulty in obtaining realistic results from a dynamic analysis.

Unfortunately, modelling of the force-deformation relations of individual elements is not so easily accomplished. Elements having essentially one mode of inelastic deformation in its overloaded state are often modelled using an elasto-plastic hysteretic relation of the type shown in Fig. 19. Since this model does not reflect such phenomena as strain hardening, stiffness degradation, and strength degradation, other more refined forms such as the bilinear and trilinear hysteretic models having degradation properties are often used. Elements having more than one mode of inelastic deformation in their overloaded condition are, of course, considerably more difficult to model realistically. One model which has been used for prismatic elements subjected to yielding due to biaxial bending and axial deformation is that shown in Fig. 20⁽¹⁰⁾. This model assumes elastic behavior for points in the three-dimensional force space lying inside the yield surface but assumes yielding of the elasto-plastic type for points which lie on the surface or move along the surface. Since force components represented by points outside the yield surface are not permitted by this model it is essentially a three-dimensional form of the elasto-plastic hysteretic model shown in Fig. 19. Obviously, extensions of this three-dimensional model to reflect strain hardening, stiffness degradation, and strength degradation are difficult to define realistically. Modelling of shear walls and certain other elements are even more difficult to model in their post yield state under cyclic conditions.

Obviously to develop realistic mathematical models of structural elements, experimental data on their dynamic force-deformation characteristics must be obtained. The Earthquake Engineering Research Center at the University of California, Berkeley, has for several years had an active experimental research program aimed at providing this information. Figure 21 shows a reinforced concrete element being subjected to pure flexure in its central region under controlled cyclic conditions⁽¹¹⁾. With good detailing of the reinforcing steel, excellent post yield performance can be achieved as shown by the large stable hysteresis loops in Fig. 22. Figure 23 shows a relatively short reinforced concrete element under conditions of flexure and high shear⁽¹²⁾. As shown in Fig. 24, the resulting load-deflection hysteresis loops have a "pinched" form due to shear deformations and bond failures occurring in the damaged regions on each side of the column stubs. The energy absorption capacity represented by areas under the hysteresis loops is therefore greatly reduced. While this particular element shows considerable degradation of stiffness, its strength is well maintained under repeated cycles of loading. Figure 25 shows a reinforced concrete element subjected to flexure, shear, and high axial load. A failure pattern for this type of specimen, when subjected to a constant axial load equal to 75 percent of the balanced point load and cycled under flexure and shear, is shown in Fig. 26. Because of the presence of the axial load, the lateral force-displacement hysteresis loops, Fig. 27, show not only an appreciable degradation of stiffness but also a rapid degradation of strength. Figure 28 shows a spandrel wall beam-column element under combined loading with the cyclic loading taking place in the transverse direction of the column.

When standard ties are used in the column a very brittle failure occurs as shown in Fig. 29⁽¹³⁾. If, however, a closely spaced spiral tie is used throughout its length and on into the spandrel beams, ductile behavior is achieved as shown in Fig. 30. In this case, the concrete outside the tie spalls off completely; however, the contained concrete within the spiral tie remains effective even under large deformation cyclic conditions. This behavior illustrates the highly beneficial effect received through effective containment of the core concrete. Obviously, selection of reinforcement details has a major influence on the force-deformation characteristics. Figure 31 shows a masonry wall element under combined loading⁽¹⁴⁾. The large coil springs shown at the top of this figure provide a constant vertical load representing dead load conditions in the prototype structure while the hydraulic actuators provide cyclic transverse loadings simulating seismic conditions. A typical shear failure pattern for this type of wall element having vertical edge reinforcing only is shown in Fig. 32 and a typical lateral force-displacement relation is shown in Fig. 33. From the failure pattern, it is clear that vertical and horizontal reinforcing distributed throughout the element would improve its force-deformation characteristics considerably.

From the above brief discussion on experimental behavior, it is clear that structural detailing, structural sizing, and form of combined loading are all important factors which must be considered when selecting appropriate mathematical models for structural elements. Also, interaction of these primary elements with secondary architectural elements should not be overlooked. For example, the sunshades shown in Fig. 34 greatly shortened the effective length of the column resulting in a brittle type failure. Keeping in mind all of these factors, it is quite evident that realistic mathematical modelling of complete structural systems is a most difficult task. Therefore, it is reasonable to assume that large variations often occur between the force-deformation characteristics of the mathematical model and the force-deformation characteristics of the prototype structure. Hopefully, continued research and improvements in seismic code provisions can reduce these variations.

Let us now turn our attention to the energy absorption characteristics of structural elements which are so important to mathematical modeling when the dynamic excitation is highly oscillatory as in the case of earthquakes. Unfortunately damping characteristics are the least known of all physical characteristics which are important to dynamic response calculations. For large cyclic excursions into the inelastic range, hysteretic forms of damping become dominant. This form of damping depends entirely upon the hysteretic force-deformation relations selected for individual structural elements. For cyclic oscillations in the elastic range, energy absorption is still present. While this form of damping usually is both velocity and displacement dependent and often is nonlinear in form, it is standard practice to model such damping assuming the linear viscous form. The coefficients assigned to this form of damping usually consist of two parts, one part proportional to the corresponding mass coefficients and one part proportional to the corresponding stiffness coefficients (Rayleigh damping) and are usually assigned numerical values consistent with damping ratios believed to be proper for the lower modes of vibration. Since experimental evidence often shows

these ratios to be nonlinear with vibration amplitude, values of the coefficients are selected to represent damping present at amplitudes between working stress levels and yield stress levels. When experimental evidence is lacking, considerable judgment must be relied upon in assigning numerical values to these coefficients. Once numerical values have been assigned in this manner, one must decide whether or not the corresponding velocity dependent forces should be permitted to act throughout the elastic and inelastic ranges of deformation. Since no sound justification can be given for permitting these forces to develop in proportion to velocities associated with the inelastic rates of deformation, it is fairly common practice in setting up mathematical models to change the stiffness proportional damping in the same manner the stiffnesses themselves change due to inelastic deformations. In other words, to the structural analyst, this means keeping the stiffness proportional damping matrix proportional to the instantaneous stiffness matrix at all times during the periods of inelastic deformation. Based on these comments, it is apparent that large variations can occur between the damping characteristics of the mathematical model and the prototype structure.

Finally to complete this discussion on mathematical modelling, a few words should be stated regarding the modelling of foundation-structure interaction which often has a significant influence on dynamic response, particularly in the case of stiff structures on moderate to soft foundations. Considering first those structures supported on spread footings or mat foundations, three basic forms of foundation modelling have been used (1) inserting discrete springs and dashpots between the structure and the soil foundation with the spring constants determined from elastic static half-space theory and the dashpot coefficients assigned values to represent material damping in the soil, (2) inserting discrete springs and dashpots between the structure and soil foundation with the spring constants and dashpot coefficients being frequency dependent in accordance with the elastic or viscoelastic dynamic half-space theory⁽¹⁵⁾, and (3) finite element representations of a body of soil at the base of the structure⁽¹⁶⁾. If the overall model of the foundation-structural system is nonlinear in form, dynamic analyses must be carried out in the time domain as a frequency domain solution is not possible. However, if the complete model is linear in form, the analysis can be carried out in either the time domain or the frequency domain, except for the second basic form which has frequency dependent parameters. In this case the solution must be carried out in the frequency domain. Unfortunately, inadequate investigations have been made to correlate the results obtained from these three basic forms. It is the author's opinion however that too often a two-dimensional plane strain finite element model is used when the structural loads are definitely transmitted into the foundation in a three-dimensional manner. If the horizontal base dimensions of the structure are similar in two orthogonal directions, the three-dimensional form of load transmission should be recognized and be modelled in some representative form.

Realistic modelling of interaction for structures supported on pile foundations is even more difficult than the above case of structures supported on spread footings or mat foundations⁽¹⁷⁾. It is clear therefore that considerably more research is needed to develop reliable methods.

THREE-DIMENSIONAL DYNAMIC ANALYSES

Three-dimensional dynamic analyses of linear systems having constant structural parameters can be carried out in either the time domain or the frequency domain⁽¹⁸⁾. Most analyses of this type carried out in the past have used the time domain approach. Recently however the frequency domain approach has become competitive due to the development of Fast Fourier Transform techniques. If frequency dependent parameters are present in the mathematical model, a time domain solution is not possible, but the frequency domain approach can be used without difficulty. Regardless of the form of solution, linear systems can be analyzed with a high level of confidence as to accuracy of results. Nonlinear systems, on the other hand, cannot be analyzed with this same high level of confidence. Experience shows that it is most difficult to get good correlations between time-history predictions of response and corresponding experimentally measured results. Figure 35 shows a simple two-story reinforced concrete structure being tested on the University of California, Berkeley, shaking table. Correlation studies carried out in this investigation verify the above statement⁽¹⁹⁾. Similar difficulties, with even greater discrepancies, have been experienced in testing the three-span bridge model shown in Fig. 36⁽²⁰⁾. It has become evident that small differences in model form or in model parameters can have a large effect on dynamic response.

Let us now turn our attention to predicting maximum dynamic response of fixed mathematical models to earthquake excitations. First consider a viscously damped single degree of freedom system using three model types (1) linear, (2) elasto-plastic, and (3) stiffness-degrading⁽²¹⁾. Subjecting these models, with the elastic period of vibration set at 2.7 seconds, to stationary filtered (Kanai filter; $\xi = 0.6$, $\omega_g = 15.6$ rad/sec) white noise excitation of fixed intensity ($S_0 = 0.0516$ ft²/sec³), the probability distribution function for maximum relative displacement can be approximated in each case by a straight line on Gumbel (Extreme Type I) plots as shown in Fig. 37. Curves 1, 2, and 3 represent elastic, elasto-plastic, and stiffness-degrading models, respectively, when the viscous damping ratio is set at 2 percent. Curves 4, 5, and 6 are the corresponding curves when the viscous damping ratio is set at 10 percent. Relative displacement can be expressed in terms of ductility factor for the non-linear models and the probability distribution can, for all cases, be expressed in terms of return period measured in number of earthquakes. The significant features of the distributions in Fig. 37 are the following: (1) The most probable maximum displacements at 0.33 on the probability distribution scale are considerably greater for those models having 2 percent of critical damping than for their corresponding models having 10 percent of critical damping; however, these values vary little from one model to another. (2) The standard deviations of maximum displacement are considerably larger for the elasto-plastic and stiffness-degrading models than for their corresponding linear models and are appreciably larger for the elasto-plastic models than for their corresponding stiffness-degrading models. (3) Increasing the viscous-damping ratio increases the standard deviations of extreme value response for each model type. What is more significant to note in this discussion is that maximum response of nonlinear systems have very large variations. These variations are caused by differences allowed in the phase angles of the harmonics present in the ground motion excitations.

Keep in mind however that these differences do not change the intensities of the excitations. If the maximum intensity of excitation to be experienced by the single degree of freedom system is also treated as a random variable, one can expect probability distributions of maximum relative displacement as shown in Fig. 38. Curves 1, and 2 are based on the maximum intensity of excitation having an Extreme Type II probability distribution while curves 3, and 4 are based on a similar distribution but with the tail of the distribution cut off to reflect a finite upper bound to the maximum intensity. The probability distribution of maximum relative displacement for a fixed intensity of excitation is assumed to be Extreme Type I with a coefficient of variation equal to 0.4 for curves 2 and 4 but is taken as a unit step function, with the step occurring at the mean value of the Extreme Type I distribution, for curves 1 and 3. The latter step function distribution corresponds to a coefficient of variation equal to zero. Since for low risk structures, we are interested in that value of maximum response corresponding to some prescribed value near one on the probability distribution scale, a final distribution corresponding to curve 4 which recognizes both intensity of excitation and maximum response as random variables should be used. For a nonlinear system, a coefficient of variation equal to 0.4 is easily possible as shown in Fig. 37; therefore, the distribution given by curve 4 is quite representative of what one could expect in a qualitative sense. It has previously been stated in the literature that only the mean value of maximum response for a fixed intensity need be considered since the intensity distribution has such a wide variation, i.e., the distribution corresponding to curve 3 can be used in predicting maximum response⁽²²⁾. Based on the above comments, it is apparent that the present author disagrees with that particular point of view.

To conclude this discussion on predicting maximum response, a few words should be stated regarding the behavior of multi-degree of freedom systems. Previous studies show that variances of maximum response for fixed mathematical models have magnitudes similar to those shown previously for single degree of freedom systems. If variances in structural properties are introduced into these models, one can expect the resulting variances in maximum response to be even greater.

INTERPRETATION OF DYNAMIC ANALYSES IN TERMS OF PROTOTYPE BEHAVIOR

Having established maximum levels of dynamic response for the mathematical model in probabilistic form, the results must be interpreted in terms of prototype performance and possible loss.

As pointed out by Sawyer⁽²³⁾, failure of a structure under increasing load generally occurs in successively more-severe stages under successively less-probable levels of load. To illustrate this point, he published the relationship given in Fig. 39 which shows failure-stage vs. load (pseudo-static type increasing monotonically) for a typical statically indeterminate reinforced concrete building and states, "The first failure stage is that caused by minor tensile cracking which almost always occurs and which causes very small loss. With higher load reinforcement yields at one, then more progressively longer regions,

leading to wide cracking, objectionable deflections, loss of user-confidence, and need for repairs. With further increases in load, spalling and crushing occur, deflections become excessive, and the building is soon evacuated. The final failure stages are the collapse of portions of the frame, followed by the limit stage of collapse of the entire frame." While this relationship is highly variable and depends very much on structural type and structural detailing, it does illustrate very well the basic concept which should be used in assessing performance and possible losses to be expected during the life of a structure⁽²⁴⁾. Due to the variability of loss for a given load (or the variability of load for a given loss), the relationship shown in Fig. 39 should be considered as representing mean values of the random variables involved. The full distribution, as represented by Fig. 40, can in some cases involve large variances.

For seismic excitation, loss relationships similar to those shown in Figs. 39 and 40 can be estimated where the load and load probability scales are changed to intensity of ground motion and intensity probability, respectively. Such relationships should include possible losses to architectural components such as the interior finish, exterior facing and windows and to mechanical equipment such as elevators. Since these losses are directly associated with inter-story drifts, expected yielding in the main structural system should be limited appropriately.

REDESIGN OF STRUCTURAL SYSTEM

The preceding sections of this paper have traced the design process through stages Nos. 1-5 in which the structure system has been designed and its predicted future performance has been analyzed. Should any deficiencies be apparent at this point, the preliminary design should be corrected appropriately. If the design changes are significant, it may be necessary to go through stages Nos. 3-5 a second time. Having arrived at an acceptable design, one can proceed to stage No. 7 of the design process.

ASSESS SAFETY OF SYSTEM AS DESIGNED

To make a final realistic assessment of the safety of a structural system as designed, one must recognize all of the uncontrollable variabilities related to such factors as ground motion intensity, ground motion characteristics, structural properties, and mathematical modeling. Since these variabilities are large, the only meaningful assessment is one involving concepts of probability. Therefore, one should attempt to establish the probability distribution function for maximum damage level (or loss) during the expected life of the structure. If the structure is designed to provide very low risk of damage or failure, e.g. nuclear power plant Category I structure, it must be designed with the intent of remaining elastic throughout its life span. The probability distribution function for maximum damage level can then be expected to be similar to that shown in Fig. 41, Type A structure. On the other hand, if the acceptable risk level is considerably lowered so that appreciable inelastic deformations are permitted under maximum credible earthquake conditions, the probability distribution function for the maximum

damage level might very well have the appearance of that shown in Fig. 42, Type B structure.

It is important to recognize the large variance associated damage level in the latter case, Fig. 42; particularly, when concerned with the safety of a large number of buildings. The probability that one structure out of a population of N will experience a maximum damage level equal to or greater than D is $[1 - P(D)]^N$. This indicates that the individual damages of buildings of similar design and construction located equal distances from an earthquake epicenter can range from no damage to heavy damage or collapse. Observations following damaging earthquakes confirm the validity of this statement.

ASSESS SAFETY OF SYSTEM AS BUILT

The previous assessment of the safety of a structural system as designed assumes that available knowledge has been applied effectively. Unfortunately, too often this is not the case as evidenced by many structural failures where the causes can be traced to errors in design or construction or to a lack of quality control. Every effort should, of course, be made to eliminate these causes.

CONCLUDING REMARKS

An attempt has been made in this paper to create a better awareness of the uncertainties involved in the seismic design process of important structures and to encourage the use of probabilistic methods in assessing seismic risk. All probability distributions presented are intended to reflect realistic statistical trends but should not be assumed accurate in a quantitative sense. Hopefully, the general discussion presented will be helpful in bringing the many problems involved in seismic design into better focus.

ACKNOWLEDGMENT

The author expresses his sincere thanks and appreciation to Professors V. V. Bertero and A. K. Chopra for their helpful comments and suggestions made during the preparation of this paper. Special thanks are also expressed to the U. S. National Science Foundation for its financial support of the research investigations referred to herein.

REFERENCES

- (1) "Managua, Nicaragua Earthquake of December 23, 1972," Earthquake Engineering Research Institute, Conference Proceedings, Vol. I, San Francisco, California, November 29-30, 1973.
- (2) Chopra, A. K., Bertero, V. V., and Mahin, S. A., "Response of the Olive View Medical Center Main Building During the San Fernando Earthquake," Proceedings of the Fifth World Conference on Earthquake Engineering, Rome, Italy, July 1973.
- (3) "Proceedings of the U.S.-Japan Seminar on Earthquake Engineering with emphasis on The Safety of School Buildings," September 21-26, 1970, Sendai, Japan, compiled by The Japan Earthquake Engineering Promotion Society, 1971.
- (4) Rosenblueth, E., "The Six Components of Earthquakes," Proceedings of the Australian and New Zealand Conference On the Planning and Design of Tall Buildings, Sydney, Australia, August 14-17, 1973.
- (5) Tsai, N. C., "Spectrum-Compatible Motions for Design Purposes," Journal of Engineering Mechanics Division, ASCE, Vol. 98, No. EM2, Proceedings Paper 8807, April 1972.
- (6) "Design Response Spectra for Seismic Design of Nuclear Power Plants," Regulatory Guide 1.60, Rev. 1, Directorate of Regulatory Standards, U.S. Atomic Energy Commission, December 1973.
- (7) "Topical Report, Seismic Analyses of Structures and Equipment for Nuclear Power Plants," BC-TOP-4-A Revision 3, Bechtel Power Corporation, San Francisco, California, November 1974.
- (8) Penzien, J., and Watabe, M., "Simulation of 3-Dimensional Earthquake Ground Motions," Bulletin of the International Institute of Seismology and Earthquake Engineering, Vol. (1974).
- (9) Schnabel, P. B., and Lysmer, J., "SHAKE, A Computer Program for Earthquake Response Analysis of Horizontally Layered Sites," Earthquake Engineering Research Center Report No. EERC 72-12, University of California, Berkeley, 1972.
- (10) Tseng, W-S, and Penzien, J., "Analytical Investigations of the Seismic Response of Long Multiple Span Highway Bridges," Earthquake Engineering Research Center Report No. EERC 73-12, University of California, Berkeley, 1972.
- (11) Bertero, V. V., Bresler, B., and Liao, H., "Stiffness Degradation of Reinforced Concrete Members Subjected to Cyclic Flexural Moments," Earthquake Engineering Research Center Report No. EERC 69-12, University of California, Berkeley, 1969.
- (12) Celebi, M., and Penzien, J., "Experimental Investigation Into the Seismic Behavior of Critical Regions of Reinforced Concrete Components as Influenced by Moment and Shear," Earthquake Engineering Research Center Report No. EERC 73-4, University of California, Berkeley 1973.

REFERENCES (Continued)

- (13) Kustu, O., and Bouwkamp, J. G., "Behavior of Reinforced Concrete Deep Beam-Column Subassemblages Under Cyclic Loads," Earthquake Engineering Research Center Report No. EERC 75-11, University of California, Berkeley, 1975.
 - (14) Mays, R. L., and Clough, R. W., "Cyclic Shear Tests on Fixed Ended Masonry Piers," ASCE National Structural Engineering Convention, New Orleans, La., Pre-print No. 2433, April 1975.
 - (15) Veletsos, A. S., and Verbic, B., "Vibration of Viscoelastic Foundations," International Journal of Earthquake Engineering and Structural Dynamics, Vol. 2, No. 1, July - September 1973.
 - (16) Lysmer, J., Udaka, T., Seed, H. B., and Hwang, R., "LUSH - A Computer Program for Complex Response Analysis of Soil-Structure Systems," Earthquake Engineering Research Center Report No. EERC 74-4, University of California, Berkeley, 1974.
 - (17) Penzien, J., "Soil-Pile Foundation Interaction," Chapter 14, "Earthquake Engineering," coordinating editor, Weigel, R. L., Prentice Hall, Inc., 1970.
 - (18) Clough, R. W., and Penzien, J., "Dynamics of Structures," McGraw-Hill, 1975.
 - (19) Hidalgo, P., "Earthquake Simulator Study of a Reinforced Concrete Frame," Earthquake Engineering Research Center Report No. EERC 74-13, University of California, Berkeley, 1974.
 - (20) Williams, D., and Godden, W. G., "Seismic Response of a Curved Highway Bridge Model," Proceedings of the Transportation Research Board Conference, U.S. Department of Transportation, December 1974.
 - (21) Penzien, J., and Liu, S. C., "Nondeterministic Analysis of Non-linear Structures Subjected to Earthquake Excitations," Proceedings of the Fourth World Conference on Earthquake Engineering, Vol. I, Sec. A-1, Santiago, Chile, 1969.
 - (22) Borges, J. F., and Castanheira, A., "Structural Safety," 2nd Edition, Laboratio Nacional de Engenharia Civil, Lisbon, Portugal, 1971.
 - (23) Sawyer, H. A., Jr., "Comprehensive Design of Reinforced Concrete Frames by Plasticity Factors," Contribution to the 9th Plenary Session of the Comité Européen du Béton, Symposium "Hyperstatique," Ankara, Turkey, September 1964.
 - (24) Tichy, M., and Vorlicek, M., "Flexural Mechanics of Reinforced Concrete," Proceedings of the International Symposium on Flexural Mechanics of Reinforced Concrete, ASCE 1965, ACI SP-12, Miami, Florida, November 10-12, 1964.
-

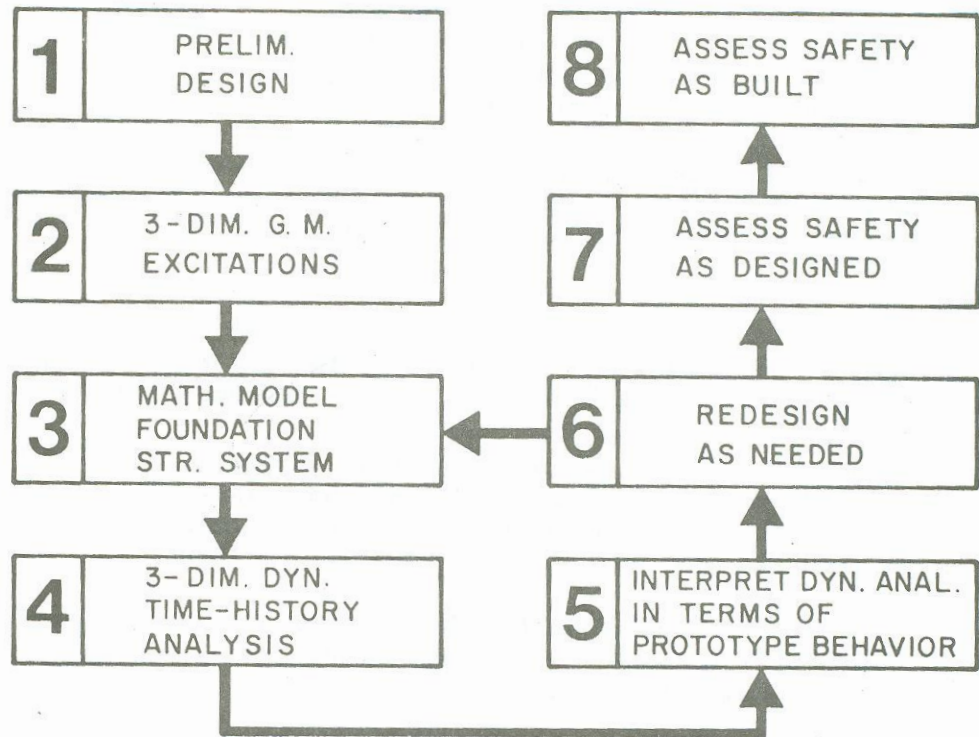


Fig. 1 The seismic design process

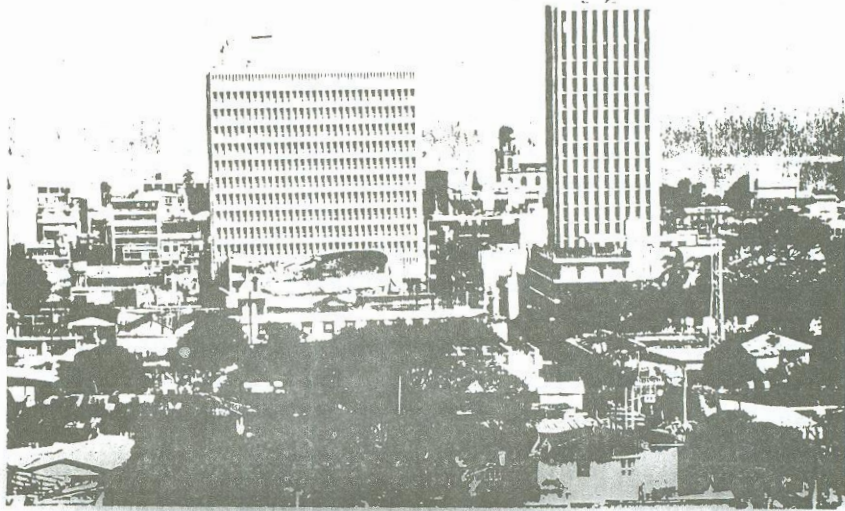


Fig. 2 Banco de America and Banco Central, Managua, Nicaragua - View No. 1

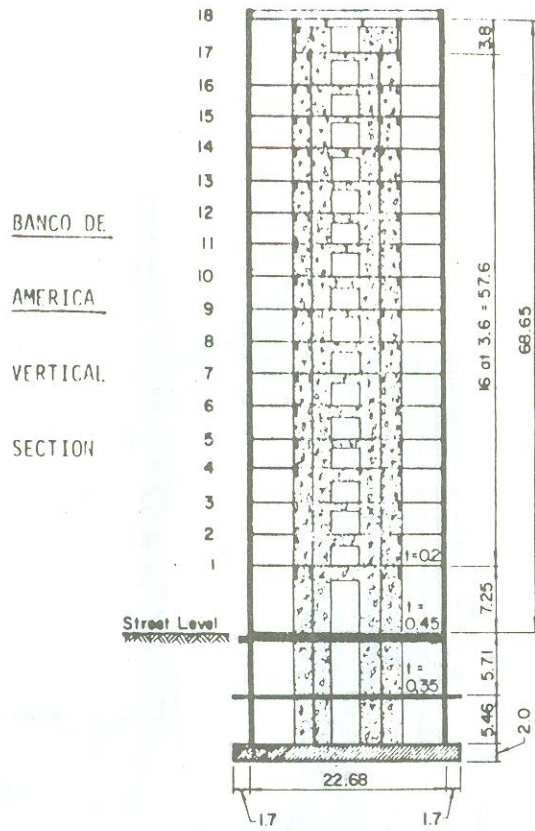
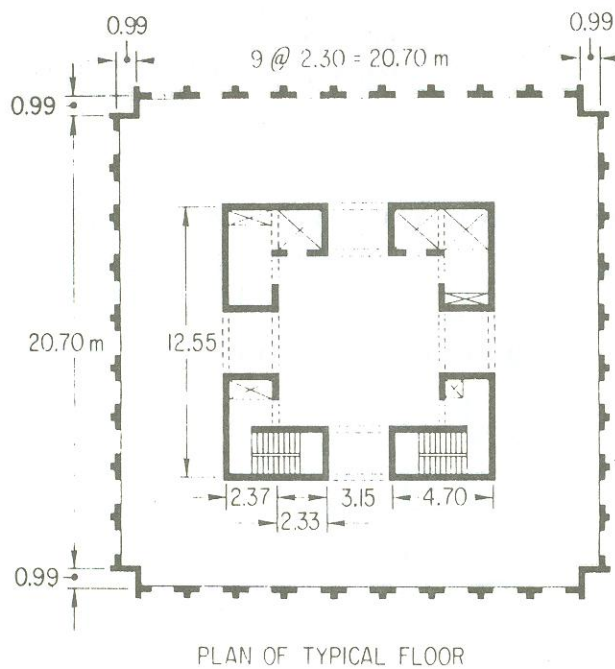


Fig. 3 Vertical section Banco de America



PLAN OF TYPICAL FLOOR
BANCO DE AMERICA NICARAGUA

Fig. 4 Plan section Banco de America

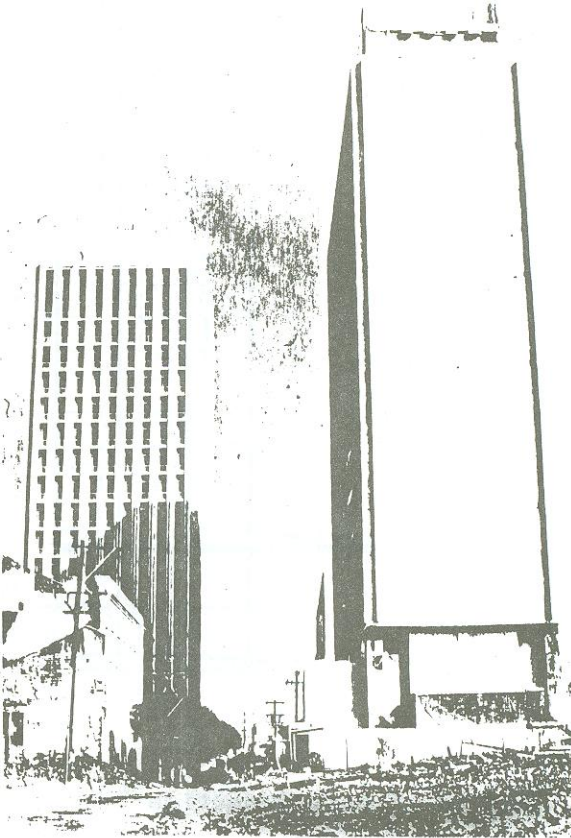


Fig. 5 Banco de America and Banco Central, Managua, Nicaragua - View No. 2

TYPICAL FLOOR PLAN ABOVE 4th FLOOR , BANCO CENTRAL

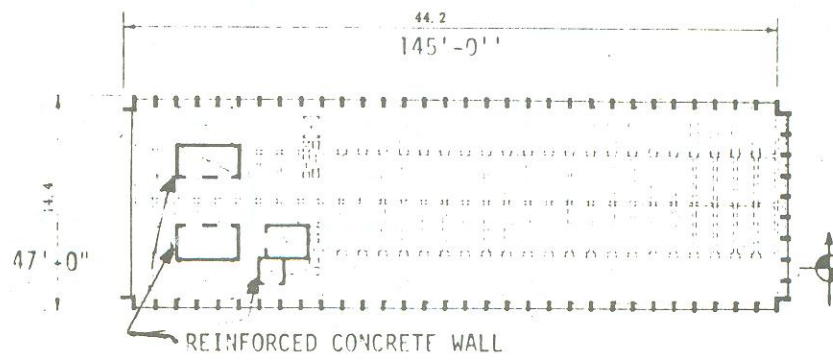


Fig. 6 Plan section Banco Central

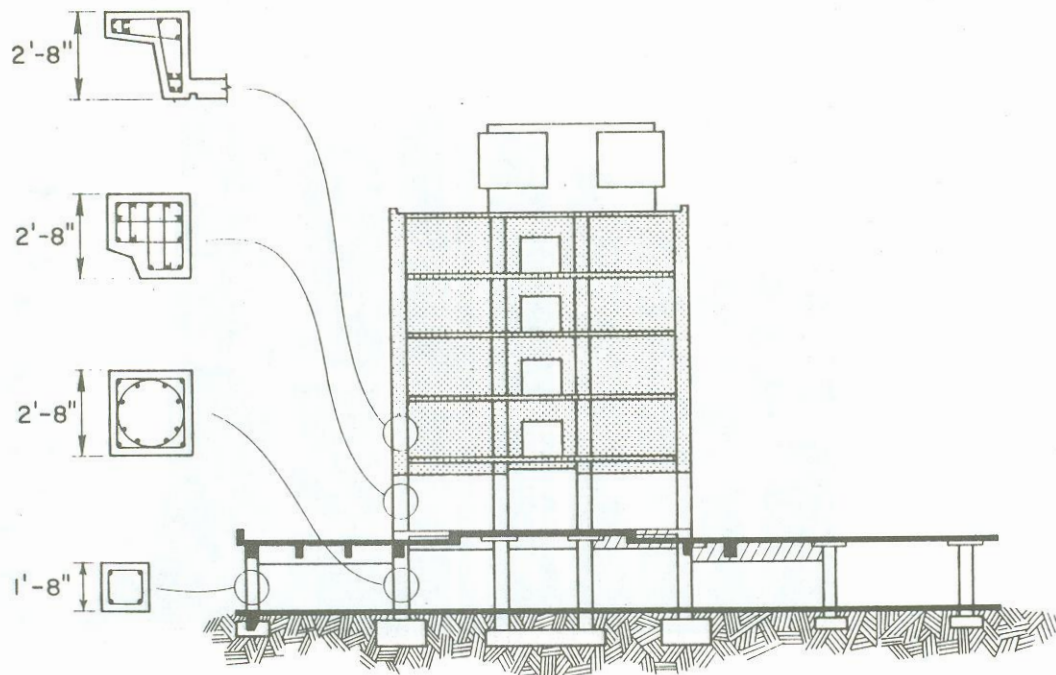


Fig. 7 Elevation Olive View Hospital -
Stiffness, Strength, and Ductility

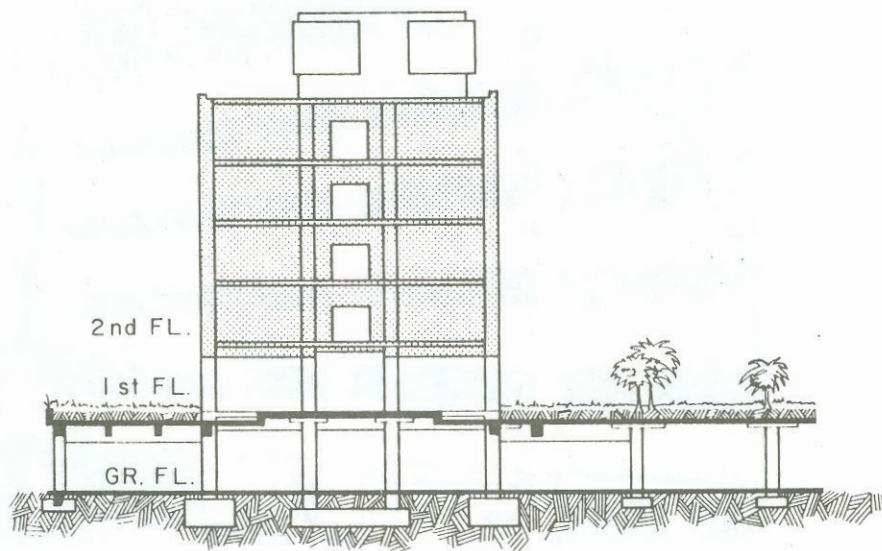


Fig. 8 Elevation Olive View Hospital - Mass

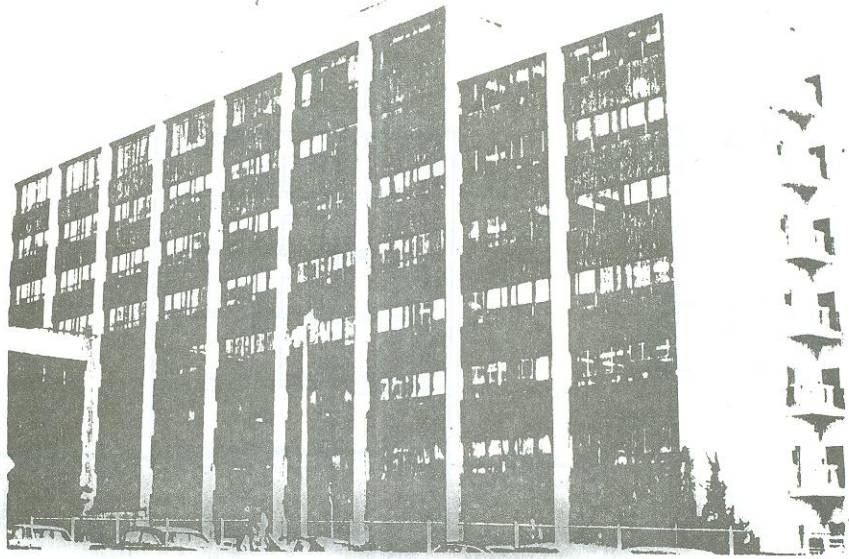


Fig. 9 Public Health Building, Berkeley, California

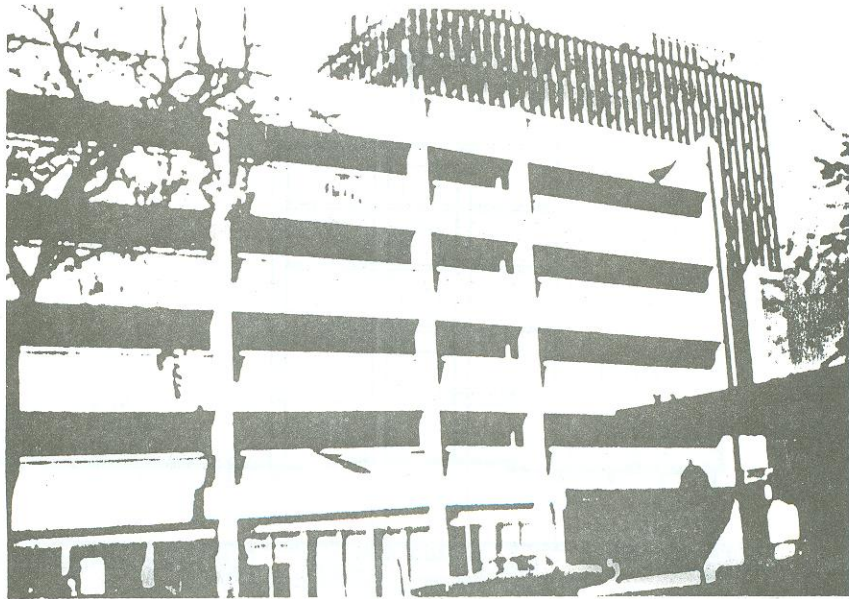


Fig. 10 Public garage, Berkeley, California

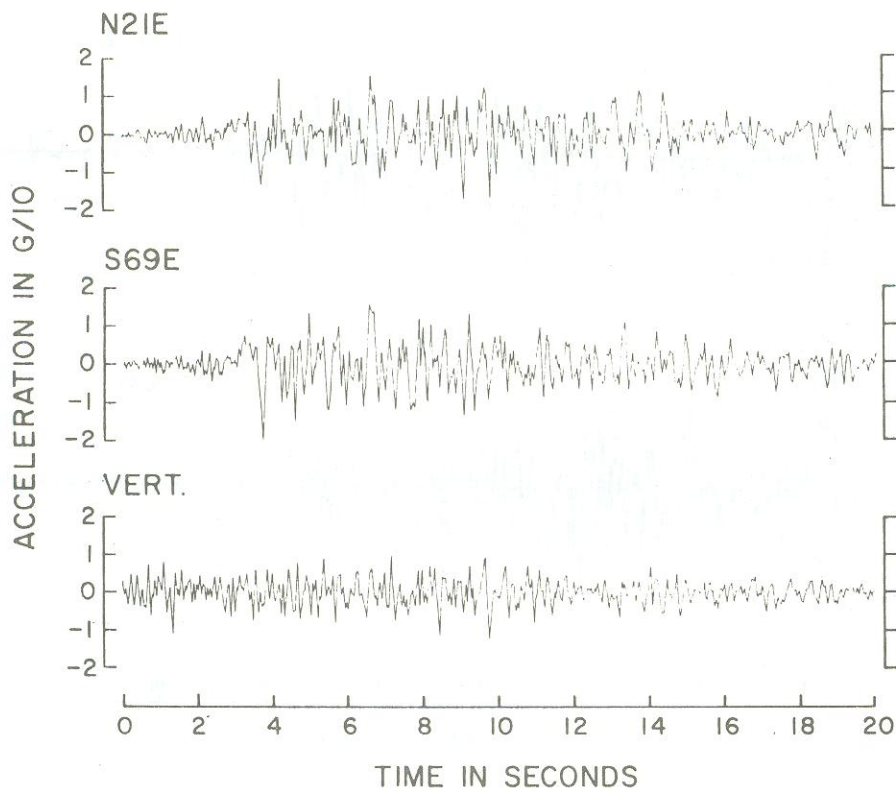


Fig. 11 Accelerograms - Taft, California, earthquake, 1952

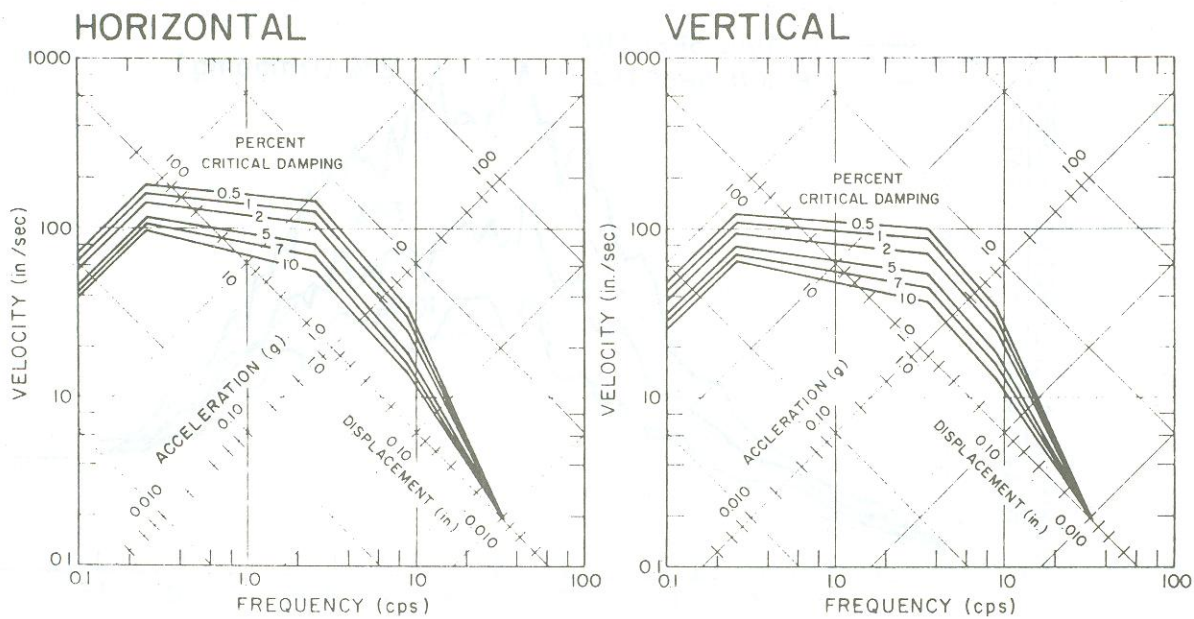


Fig. 12 Smooth design response spectrum curves (mean + 1σ levels) normalized to 1g peak ground acceleration

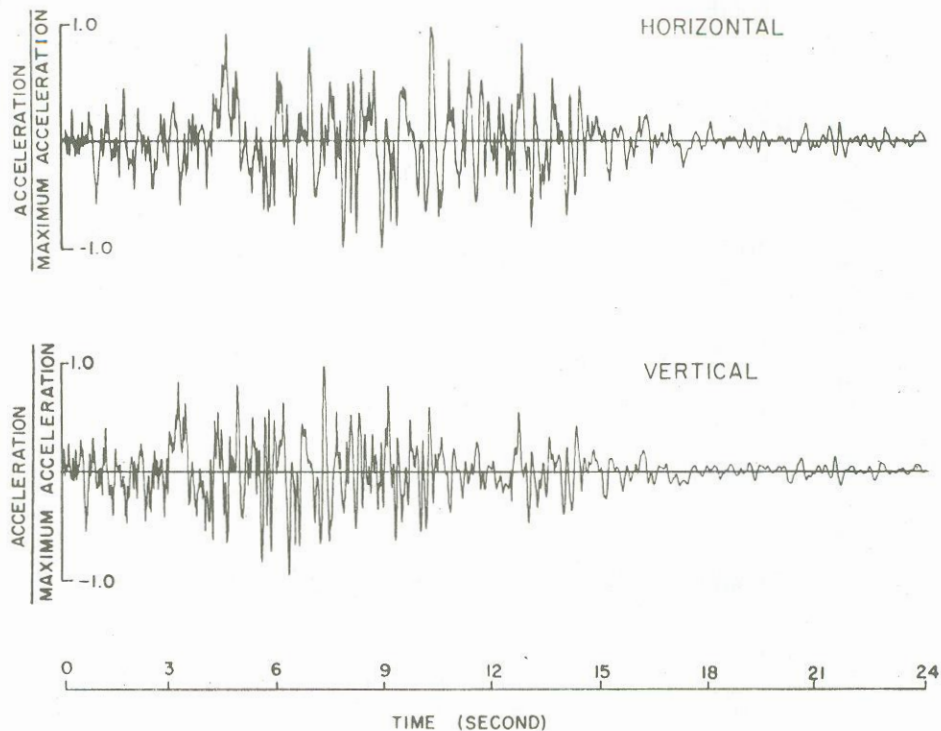


Fig. 13 Synthetic accelerograms representing smooth design response spectrum curves

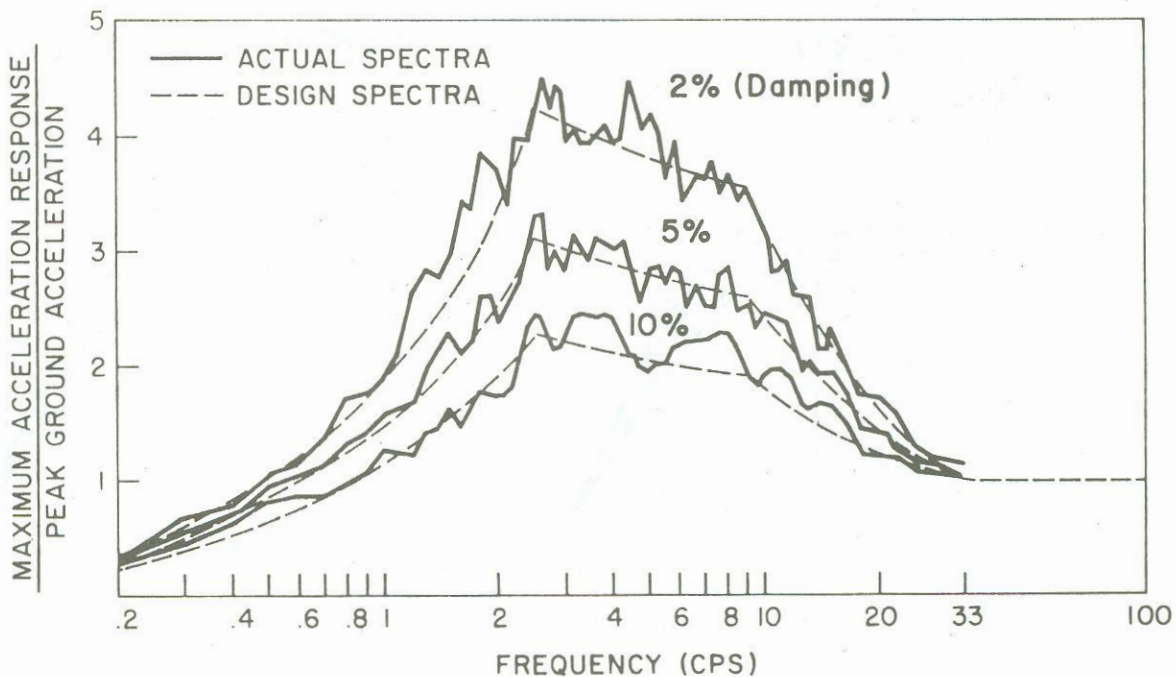


Fig. 14 Actual response spectrum curves of synthetic accelerogram for horizontal motion

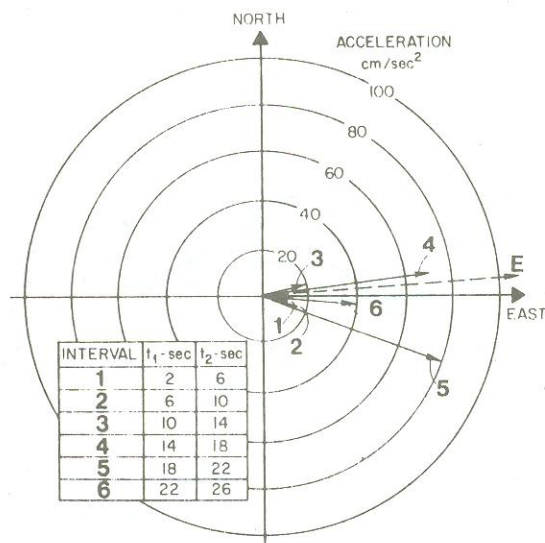


Fig. 15 Directions of major principal axis of ground motion - Tokachi-oki, Japan, earthquake (Hachinohe Station), May 16, 1968

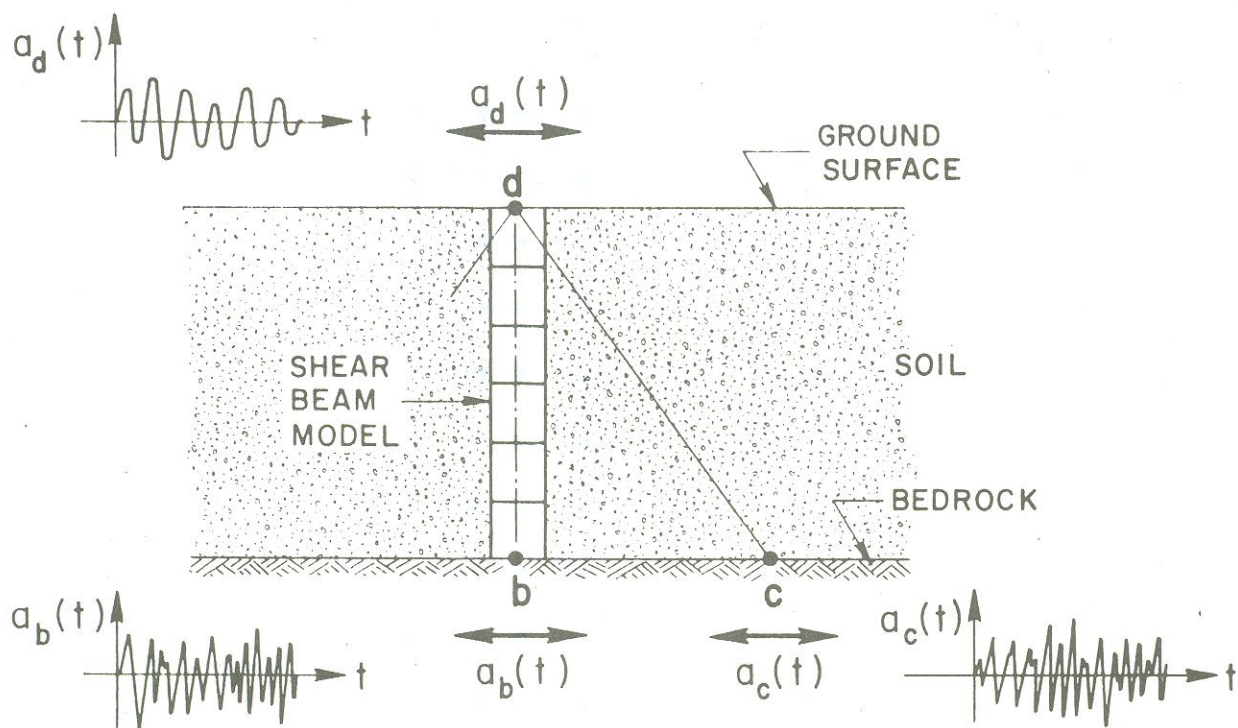


Fig. 16 The shear beam model used for soil response analyses

 RANGE OF PREDICTED RESPONSE SPECTRAL VALUES

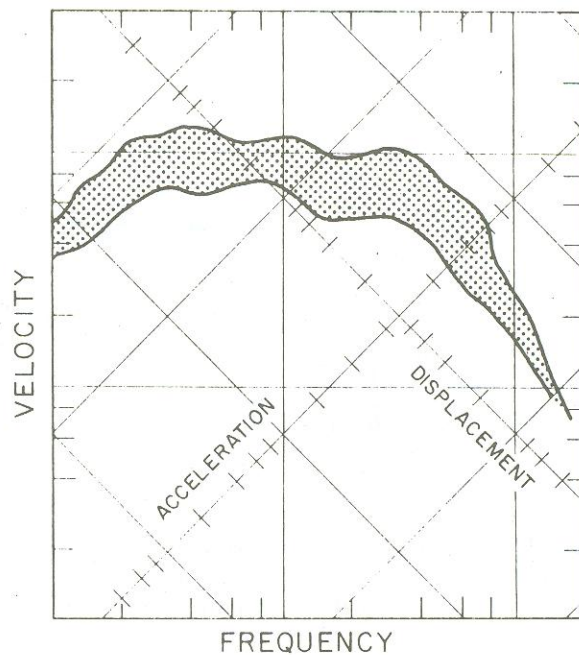


Fig. 17 Range of predicted response spectrum curves for a given site

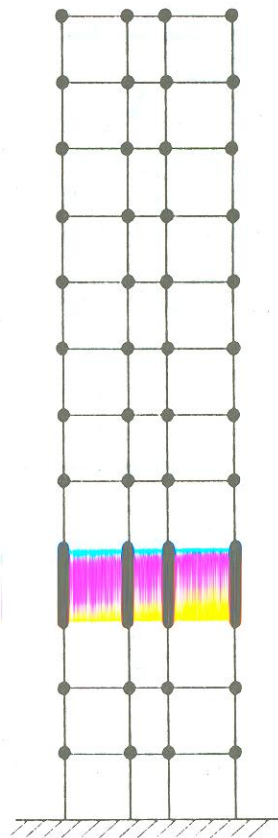


Fig. 18 Lumped mass modelling of building

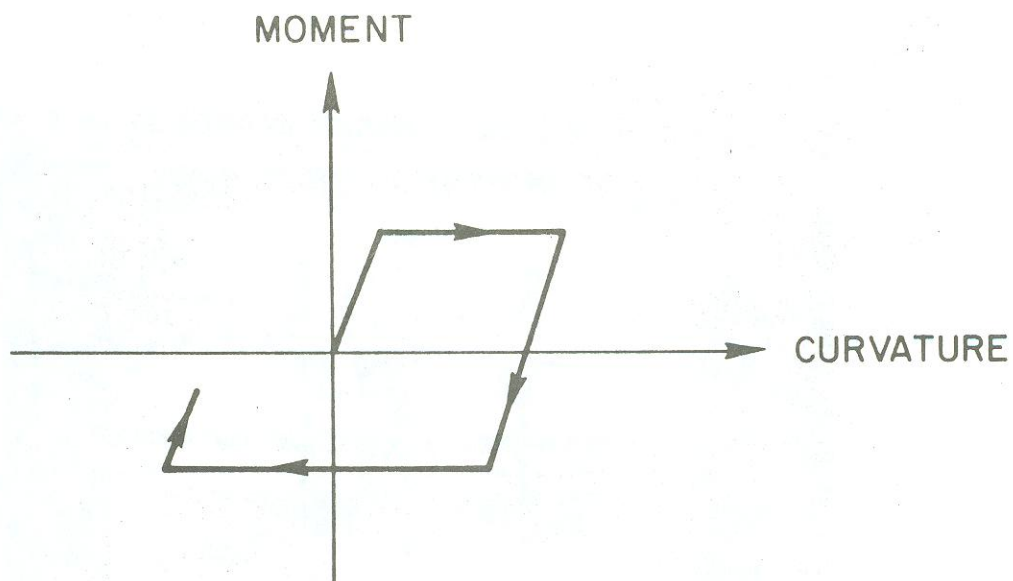


Fig. 19 One-dimensional elasto-plastic modelling of a prismatic structural element

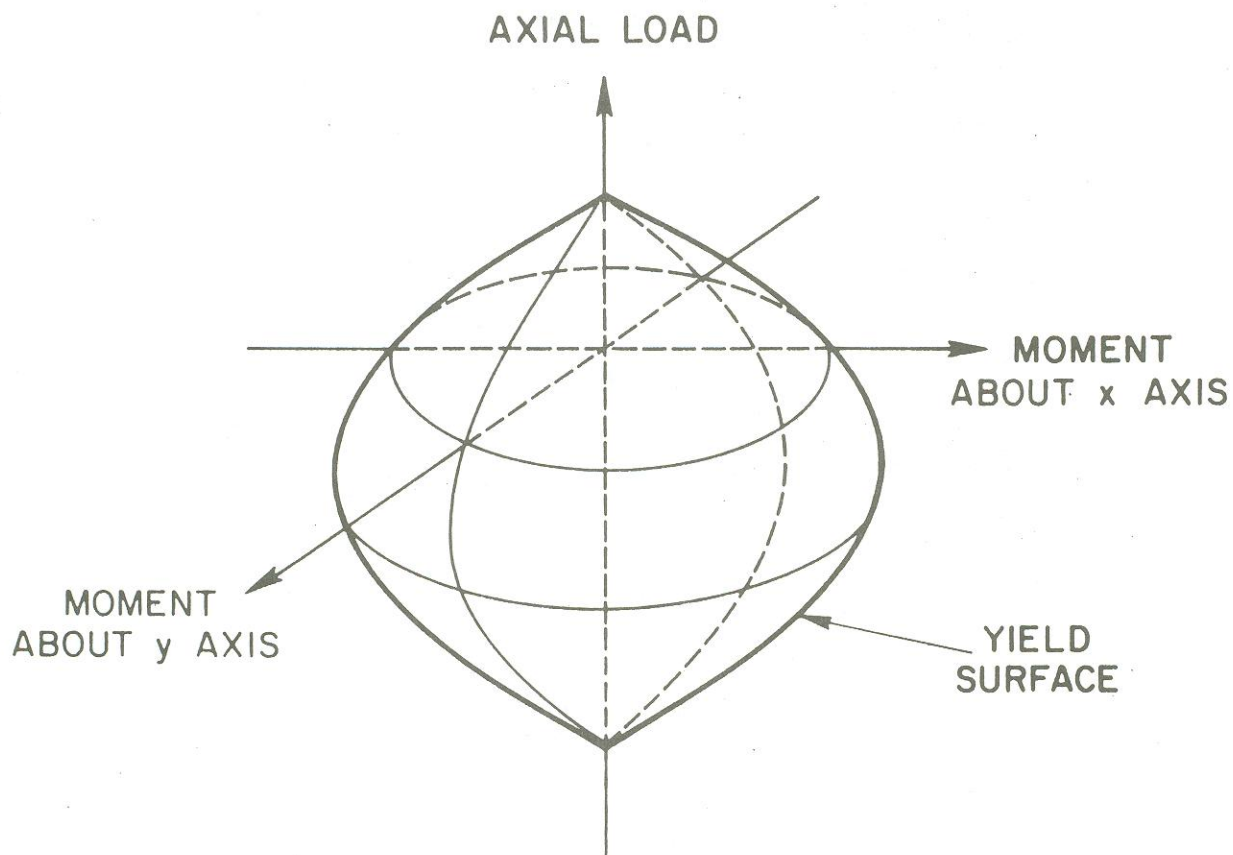


Fig. 20 Three-dimensional elasto-plastic modelling of a prismatic structural element

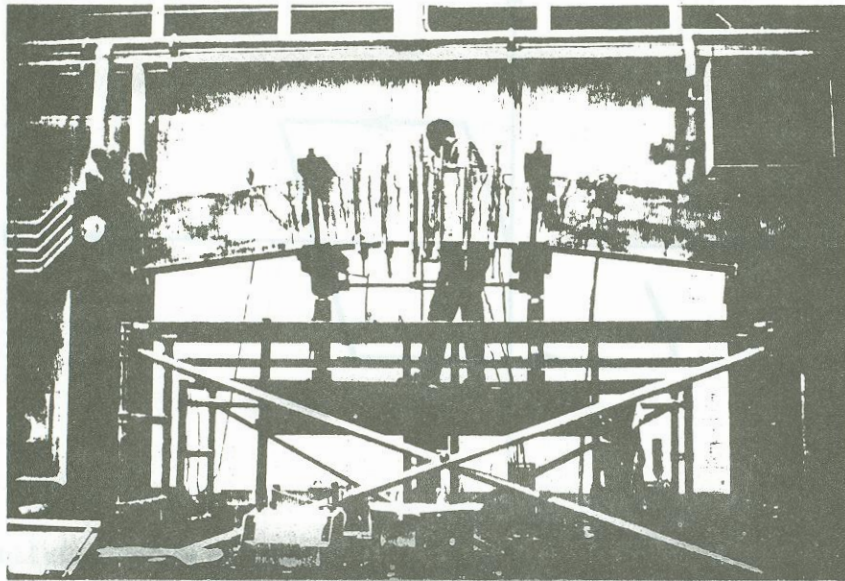
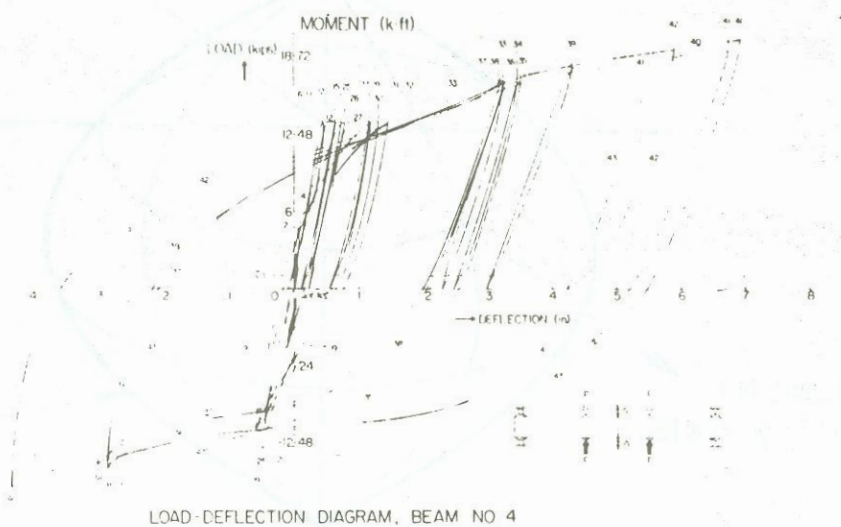


Fig. 21 Reinforced concrete element under pure flexure



LOAD-DEFLECTION DIAGRAM, BEAM NO 4

Fig. 22 Load-deflection hysteresis loops for reinforced concrete element under pure flexure

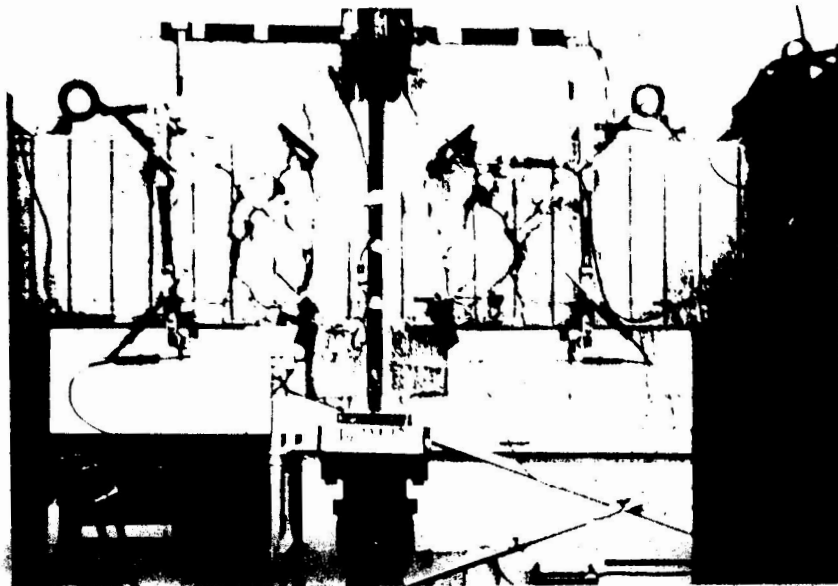


Fig. 23 Reinforced concrete element under flexure and high shear

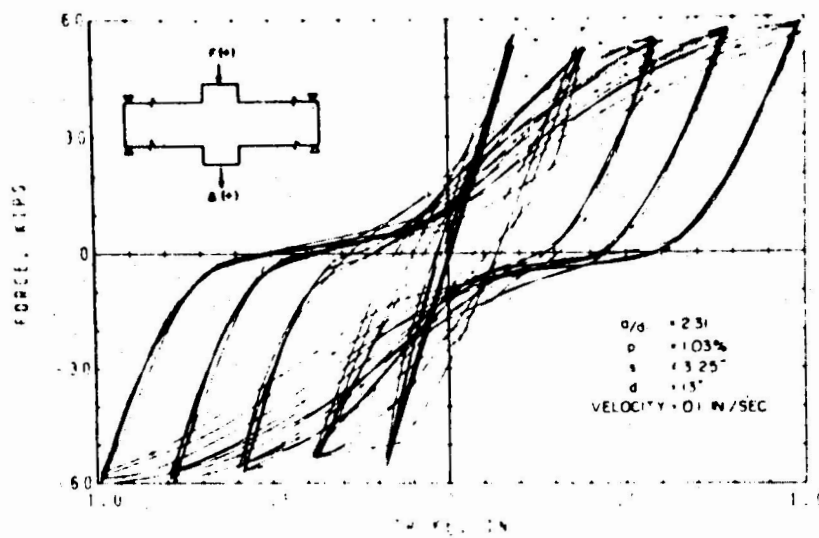


Fig. 24 Load-deflection hysteresis loops for reinforced concrete element under flexure and high shear

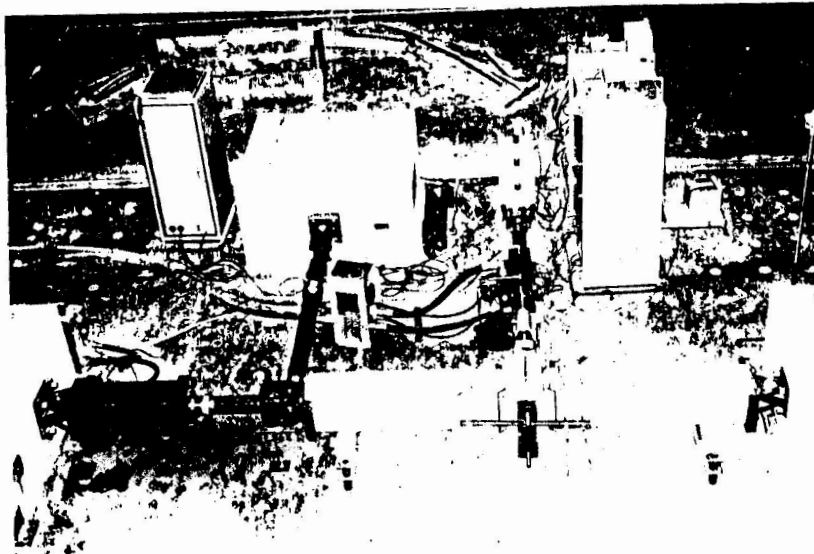


Fig. 25 Reinforced concrete element under flexure, shear, and high axial load

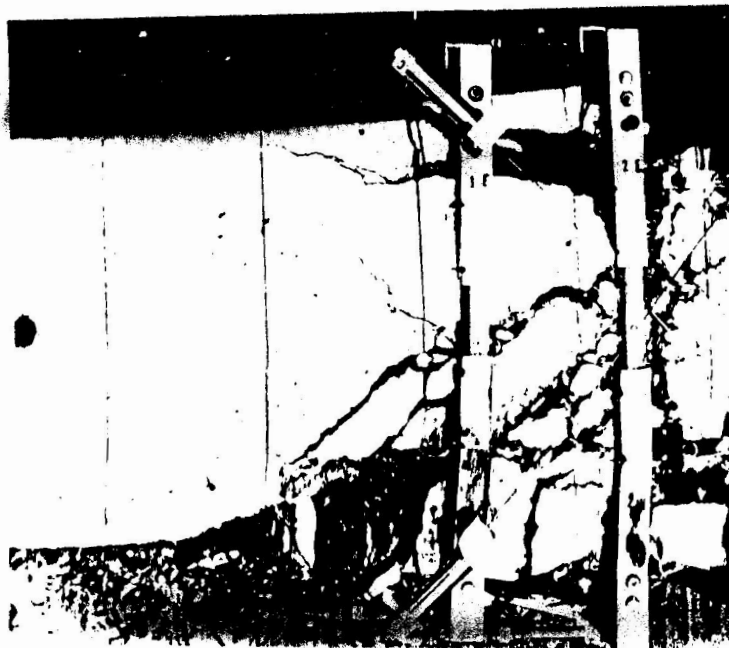


Fig. 26 Damage pattern of reinforced concrete element under flexure, shear, and high axial load

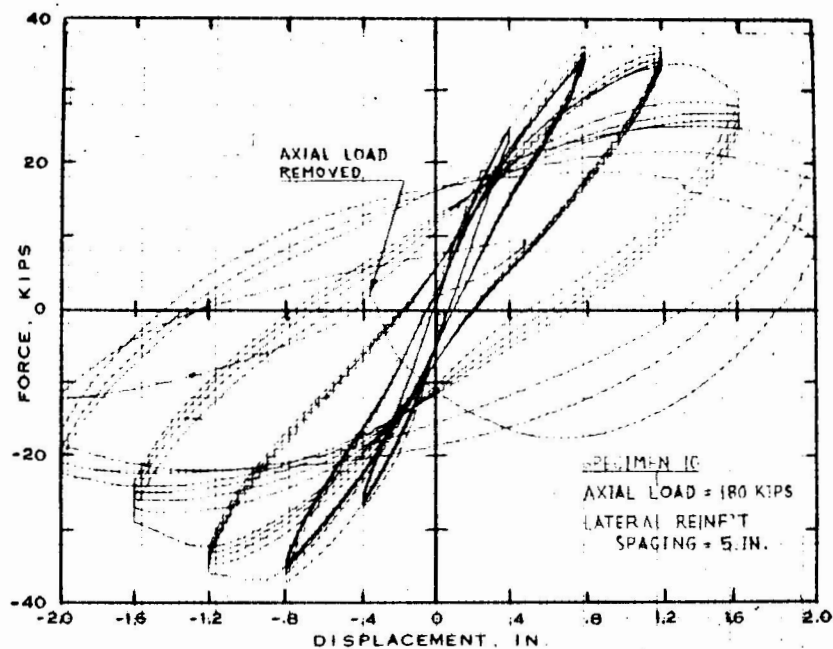


Fig. 27 Load-deflection hysteresis loops for reinforced concrete element under flexure, shear, and high axial load

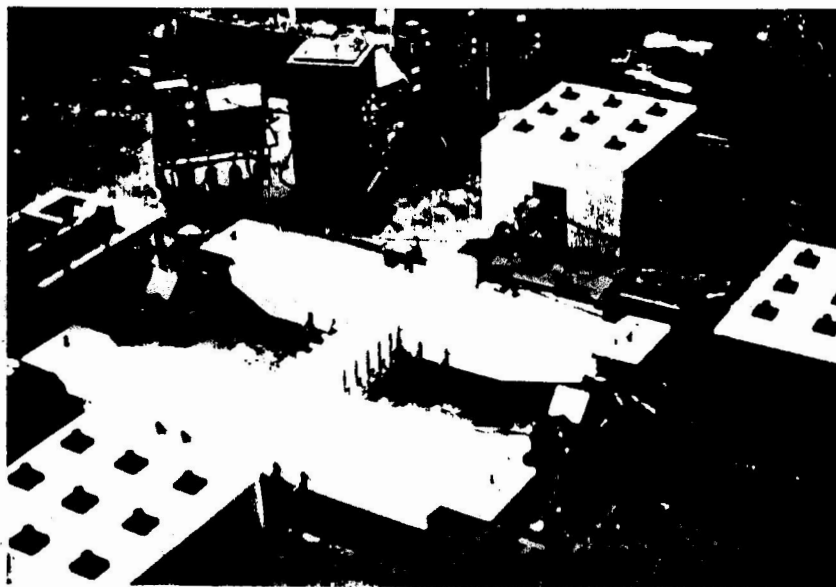


Fig. 28 Spandrel beam-column element under combined loading

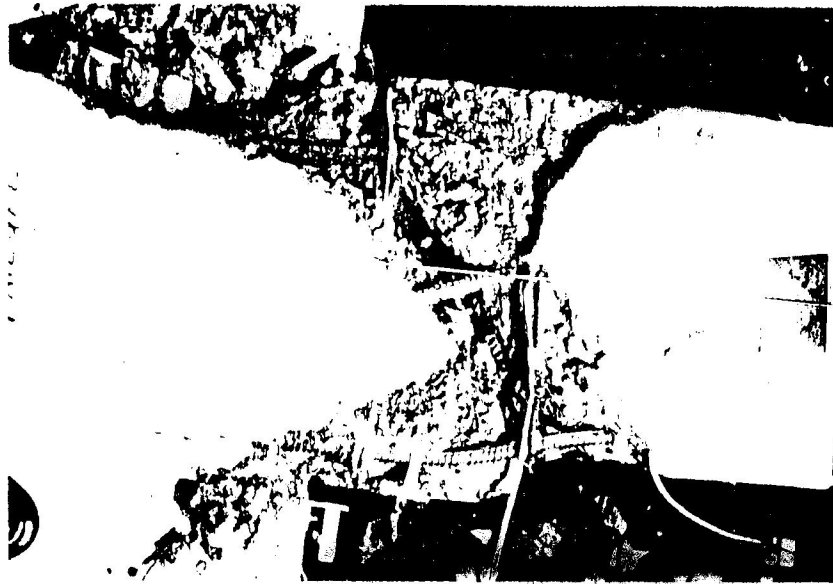


Fig. 29 Failure pattern of spandrel beam-column element - Standard ties

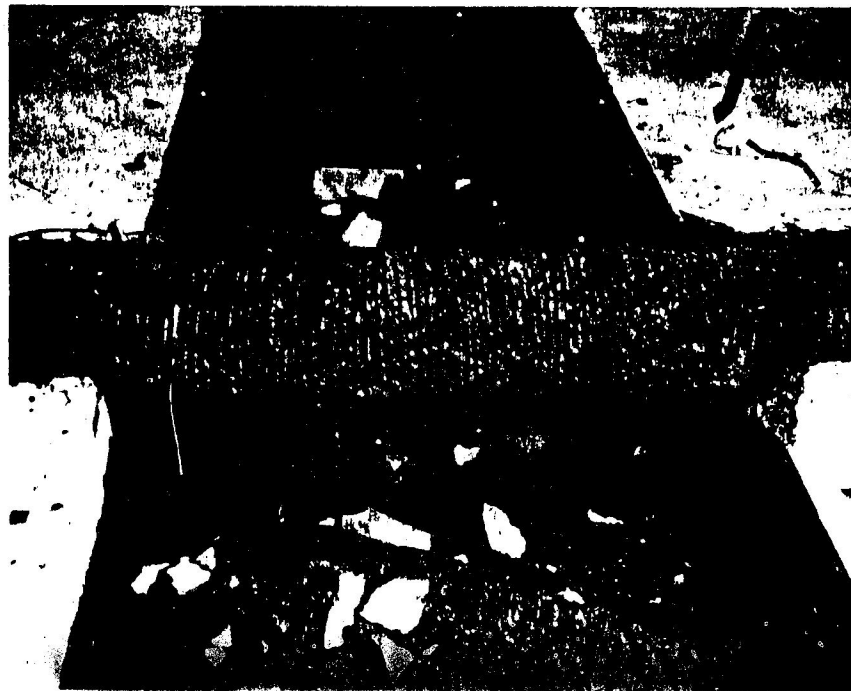


Fig. 30 Failure pattern of spandrel beam-column element - Spiral ties



Fig. 31 Masonry wall element under combined loading



Fig. 32 Failure pattern of masonry wall element

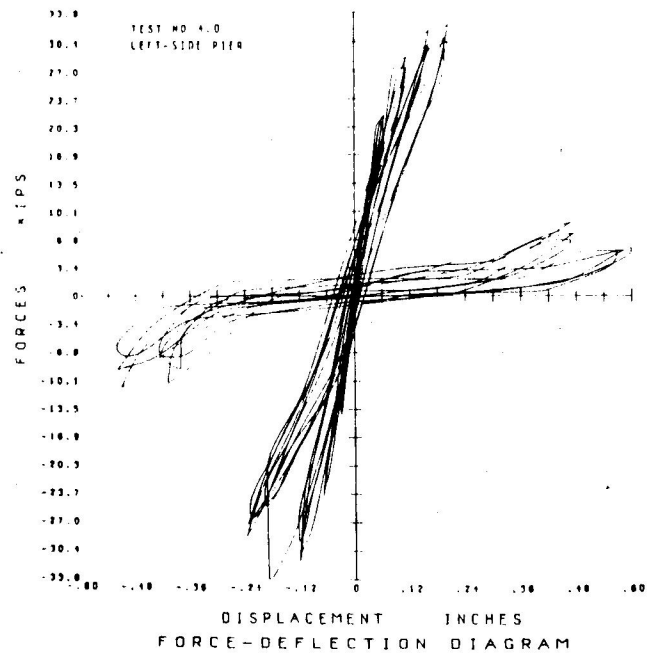


Fig. 33 Load-deflection hysteresis loops of masonry wall element

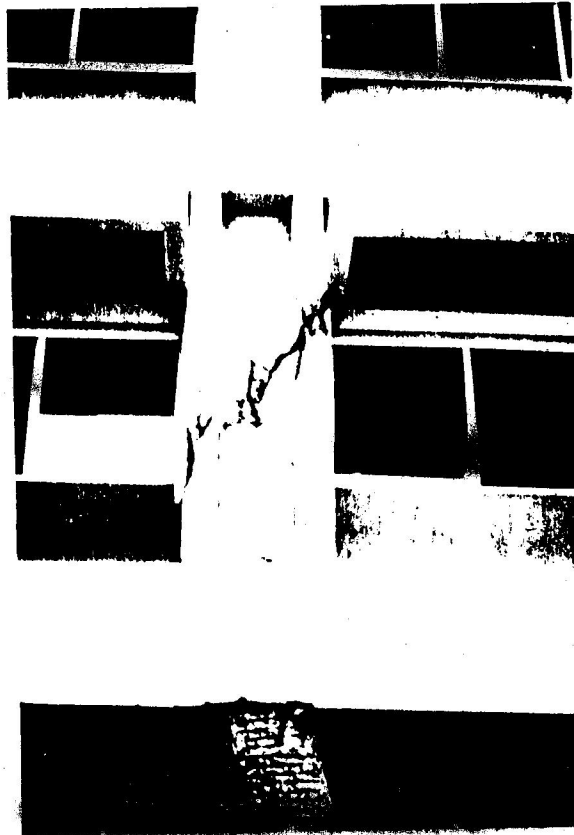


Fig. 34 Brittle column failure of short column

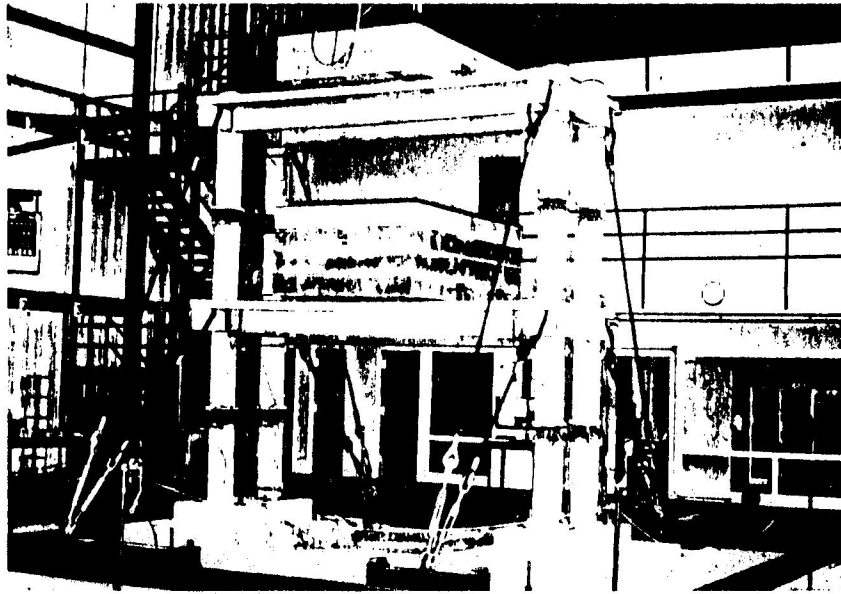


Fig. 35 Two-story reinforced concrete frame on shaking table

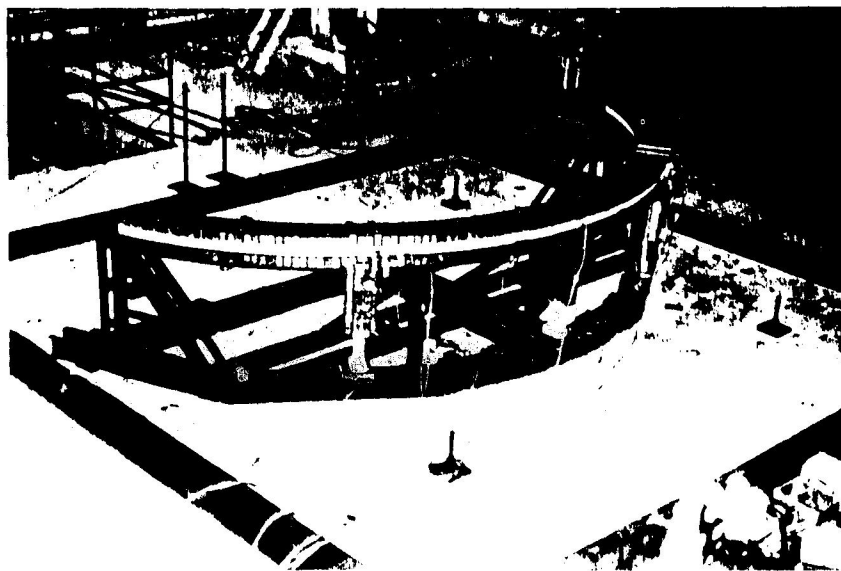


Fig. 36 Bridge model on shaking table

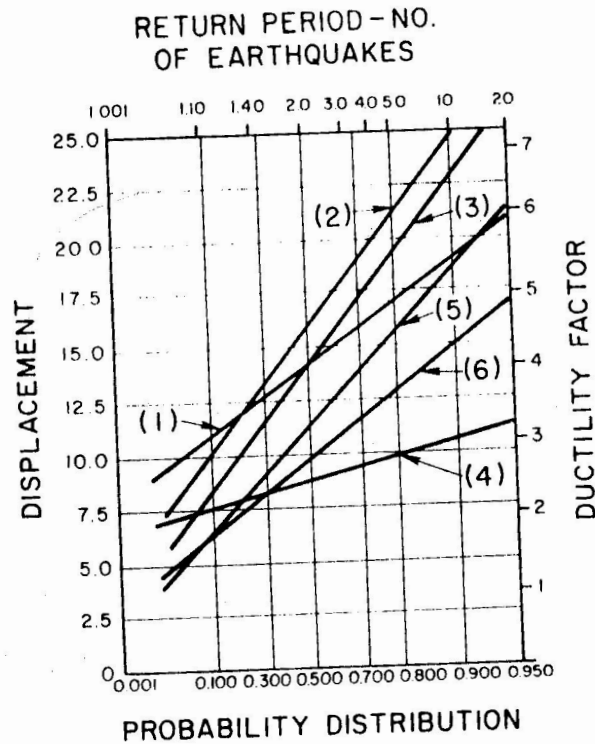


Fig. 37 Probability distribution of maximum response for single degree of freedom systems subjected to ground accelerations of fixed intensity

	STR. RESPONSE	G. M. INTENSITY
(1)	MEAN VALUE	EXTREME TYPE II
(2)	EXTREME TYPE I ($c_v = 0.4$)	EXTREME TYPE II
(3)	MEAN VALUE	UPPER BOUNDED
(4)	EXTREME TYPE I ($c_v = 0.4$)	UPPER BOUNDED

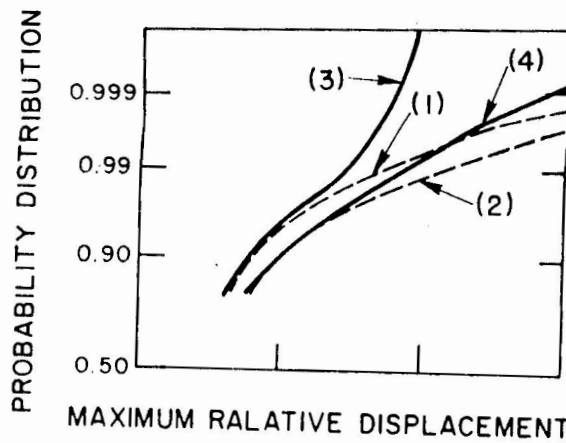


Fig. 38 Probability distribution of maximum response for single degree of freedom systems subjected to ground accelerations of variable intensity

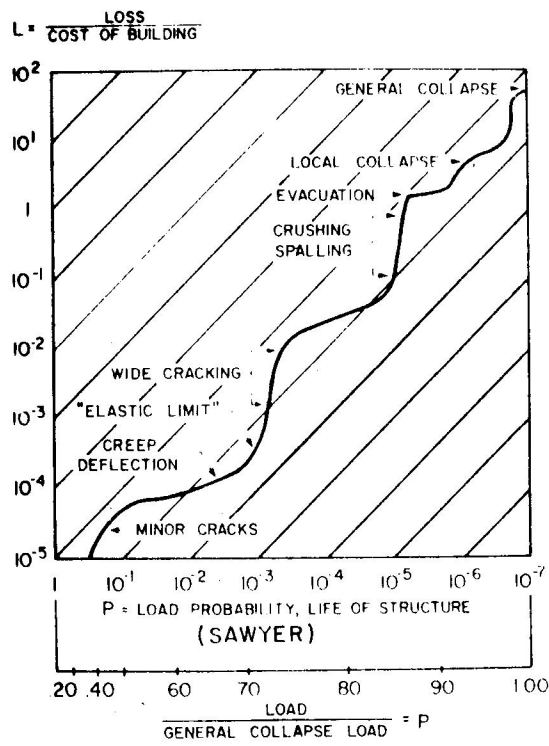


Fig. 39. Assessment of mean losses versus load probabilities during the life of structure

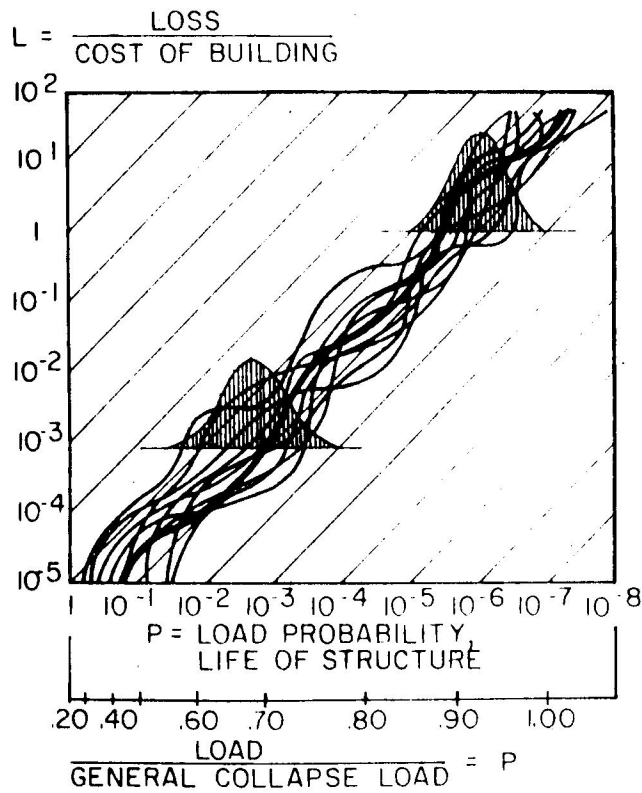


Fig. 40 Distribution of losses versus load probabilities during the life of structure

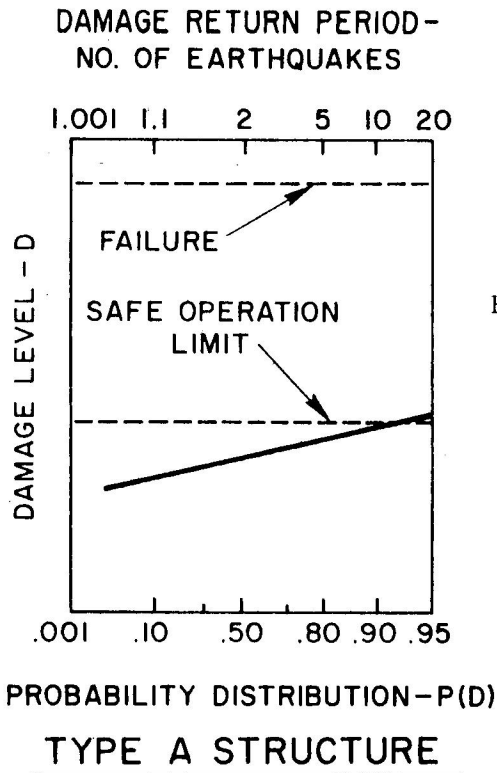


Fig. 41 Probability distribution of maximum damage level during life of structure - Type A structure

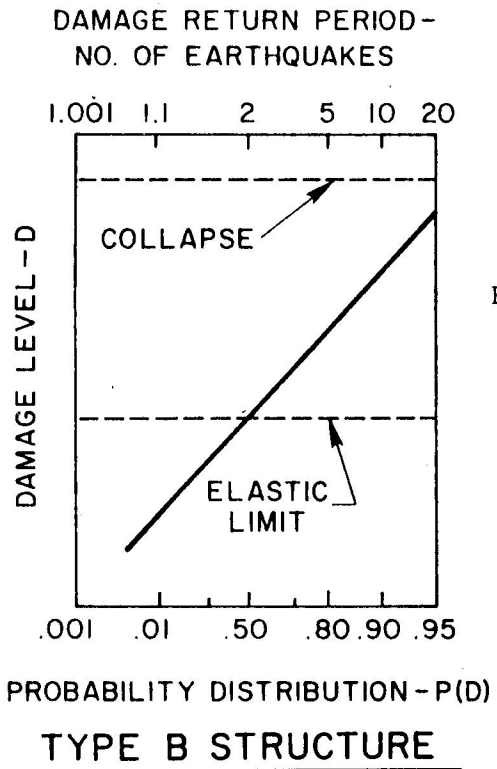


Fig. 42 Probability distribution of maximum damage level during life of structure - Type B structure